Relativistic nucleon-nucleon interaction consisting of an attractive scalar and a repulsive vector

Y. Nogami and F. M. Toyama*
Department of Physics, McMaster University, Hamilton, Ontario, Canada L8S 4M1
(Received 28 March 1988)

Relativistic models which simulate the two-nucleon system are constructed by means of the one-dimensional two-body Dirac equation, and differences between relativistic and nonrelativistic descriptions are illustrated. The relativistic interaction is assumed to consist of a Lorentz scalar S and the zeroth-component V of a vector; the S is attractive and the V repulsive. This interaction has intriguing features. Unlike the nonrelativistic case, the nucleon-nucleon phase shift can be fitted easily without assuming that the range of the repulsive V is smaller than that of the attractive S. Implications for deuteron structure are examined.

I. INTRODUCTION

There are a number of realistic nucleon-nucleon (NN) potentials which are to be used in the nonrelativistic Schrödinger equation. These potentials are realistic in the sense that they describe the NN scattering very well up to a few hundred MeV and also reproduce the deuteron binding energy. Although they differ in detail, these potentials have one feature in common; they are attractive at large to medium distances and repulsive at short distances. The short-range repulsion is required by the empirical S-wave phase shifts which change sign from positive to negative as the energy of the NN system increases. In interpreting this feature of the potentials one usually associates the repulsion with the exchange of a vector meson and the attraction with the exchange of something which effectively behaves like a scalar meson.[1] The masses of the exchanged mesons are then related to the ranges of the corresponding parts of the interaction.

The purpose of this paper is to construct relativistic models which simulate the deuteron and the $^3S_1$ NN scattering and thereby examine differences between relativistic and nonrelativistic descriptions. For the relativistic models we use the two-body Dirac equation in one space dimension.[2–4] Apart from spin-related effects, this equation amply illustrates characteristics of the relativistic description. For the two-body interaction we assume a combination of a Lorentz scalar S and the zeroth component V of a Lorentz vector; the S is attractive and the V repulsive. This particular combination of S and V, which is strongly hinted at by the recent success of the Dirac phenomenology,[5] has some remarkable features. The two-body Dirac equation can be reduced to a Schrödinger-like equation with an effective potential which we denote by W. The W that stems from the combination of S and V mentioned above turns out to be strongly energy dependent, and is very different from the traditional nonrelativistic NN potentials. The range of the repulsive V does not have to be shorter than that of the attractive S. The structure of the simulated deuteron can be appreciably different between the relativistic and nonrelativistic models.

In Sec. II we present our relativistic model based on the one-dimensional two-body Dirac equation. We also specify the nonrelativistic model with which we compare the relativistic model. In Sec. III we present the results of simulation of the $^3S_1$ NN state which contains the deuteron. Discussions constitute Sec. IV.

II. MODELS

The two-body Dirac equation reads, in natural units,

$$H\psi=E\psi, \quad H=H_1+H_2+U \ , \tag{2.1}$$

where H_i is the free Dirac Hamiltonian for particle i $(=1,2)$. Unless otherwise mentioned, we use the same notation as in Ref. 2. In the one-dimensional version that we employ, $H_i=\alpha_i p_i+\beta_i m$. For the Lorentz character of the interaction there are three parity-conserving types; scalar, vector, and pseudoscalar. In this paper we consider only scalar S and vector V, i.e., we assume that the potential U is of the form

$$U=\beta_1\beta_2 S(x)+(1-\alpha_1\alpha_2)V(x) \ , \tag{2.2}$$

where $x=x_1-x_2$ is the relative coordinate. The functions $S(x)$ and $V(x)$ correspond to $f_S(x)$ and $f_V(x)/2$ of Ref. 2, respectively. Note that the total momentum $P=p_1+p_2$ is a constant of the motion. Throughout this paper we confine ourselves to the center of mass system, i.e., $P=0$.

The wave function ψ has four components. Equation (2.1) can be reduced to an equation for one of the components of ψ, which we choose to be ϕ_2 defined in Ref. 2. We then obtain

$$\left[p\frac{4}{E+S-2V}p+S+2V+\frac{4m^2}{E-S}-E\right]\phi_2=0 \ . \tag{2.3}$$

 ©1988 The American Physical Society

We will set up the interaction such that there is a bound state which simulates the deuteron. The density in the bound state is given by

$$\rho=\sum_{i=1,4}|\phi_i|^2 = \left[1+\left[\frac{2m}{E-S}\right]^2\right]|\phi_2|^2+\frac{4}{(E+S-2V)^2}\left|\frac{d\phi_2}{dx}\right|^2 . \tag{2.4}$$

If we define χ by

$$\chi=(E+S-2V)^{-1/2}\phi_2 , \tag{2.5}$$

Eq. (2.3) can be reduced to the following Schrödinger-like equation:

$$\left[\frac{p^2}{m}+W\right]\chi=\left[\frac{E^2}{4m}-m\right]\chi , \tag{2.6}$$

where W is an energy-dependent potential defined by

$$W=\frac{1}{m}(E+S-2V)^{1/2}\frac{d^2}{dx^2}(E+S-2V)^{-1/2} +\frac{2mS}{E-S}+\left[1-\frac{2m^2}{E(E-S)}\right]\frac{EV}{m}+\frac{1}{4m}(S^2-4V^2) . \tag{2.7}$$

In the limit of very large m, Eq. (2.6) reduces to the Schrödinger equation with potential $W=S+V$.

For $S(x)$ and $V(x)$ we assume

$$S(x)=-g_S e^{-(x/a_S)^2}, \quad V(x)=g_V e^{-(x/a_V)^2} . \tag{2.8}$$

For the range parameters we (arbitrarily) keep a_S fixed at $5m^{-1}$ while we try two values for a_V, $3m^{-1}$ and $5m^{-1}$. Note that if $m=1$ GeV, $1m^{-1}\approx 0.2$ fm. In choosing the values of the strength parameters g_S and g_V, we impose two constraints:

(a) There is a bound state with binding energy $B=2\times 10^{-3}m$. For $m=1$ GeV, $B=2$ MeV, and this bound state simulates the deuteron.[6]

(b) The scattering phase shift changes sign from positive to negative at the center of mass kinetic energy of $\gtrsim 0.15m$.[7] In this way we simulate the $^3S_1$ NN phase shift.

We compare the results of our relativistic model with those of the nonrelativistic model with a potential of the form

$$U_{\rm NR}(x)=h_R\theta(b_R-|x|) -h_A e^{-(x/b_A)^2}\theta(|x|-b_R) , \tag{2.9}$$

where $\theta(x)=1$ (0) if $x>0$ (<0) and the subscripts A and R refer to the attractive and repulsive parts, respectively. We tried various different forms such as a potential with two Gaussian terms, but without any noteworthy difference.

TABLE I. Parameters of the relativistic potential of Eq. (2.8). The units are mass m for g and m^{-1} for a. The range of the attractive part $a_S=5m^{-1}$ is common to all models. Parity refers to the parity of the solutions used for simulation.

Model	Parity	g_S	a_V	g_V
A	odd	0.37	3	0.464 87
B	odd	0.8	5	0.386 82
A'	even	0.035	3	0.036 635
B'	even	0.05	5	0.037 634

III. SIMULATION

In one dimension there are two "partial waves," with even and odd parity.[7] Although it may sound odd, we prefer the odd-parity state for simulating the S state of the NN system. If we denote the Schrödinger wave function for an S state in three dimensions by $\psi(r)$, the function $u(r)=r\psi(r)$ obeys an equation which is identical to the Schrödinger equation in one dimension and the boundary condition on $u(r)$ at the origin, i.e., $u(0)=0$, is the same as that for the odd-parity wave function in one dimension. A similar situation holds for the two-body Dirac equation. For completeness we will also try (rather unsuccessfully) to simulate the NN system by means of the even-parity state of the one-dimensional model.

For the odd-parity state we consider three models, two (designated by A and B) are relativistic and the third one (C) is nonrelativistic. The corresponding models with the even-parity state are designated by A', B', and C', respectively. The parameters of the potentials of the relativistic models are listed in Table I, and those of the nonrelativistic models in Table II. Note that, in models A and A', S and V have different ranges, whereas in models B and B' the ranges of S and V are equal. The strength of the potential, in particular g_S of model B, is very large. This can be reduced by choosing a larger range. The nonrelativistic potentials in models C and C' of course consist of short-range repulsion and long-range attraction. The range of the attractive part is assumed to be the same as that of S of the relativistic models.

Let us begin with the simulation by means of the odd-parity state. Figure 1 shows the scattering phase shifts for models A, B, and C. They are all very similar to each other and to the empirical $^3S_1$ NN phase shift. These phase shifts start with π at the threshold $E=2m$ and de-

TABLE II. The parameters of the nonrelativistic potential of Eq. (2.9). The units are mass m for h and m^{-1} for b. The range of the attractive part $b_A=5m^{-1}$ is common to the two models. Parity refers to the parity of the solutions used for simulation.

Model	Parity	h_A	b_R	h_R
C	odd	0.278	2.5	2.1186
C'	even	0.0252	0.15	0.362 02

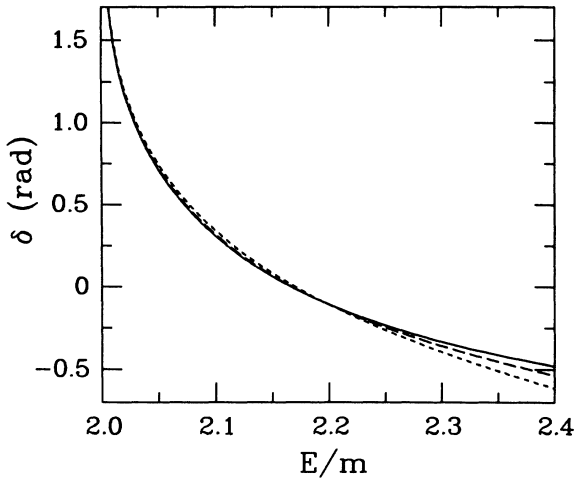

FIG. 1. The odd-parity phase shift $\delta(E)$. The solid, dashed, and short-dashed lines are for models A, B, and C, respectively.

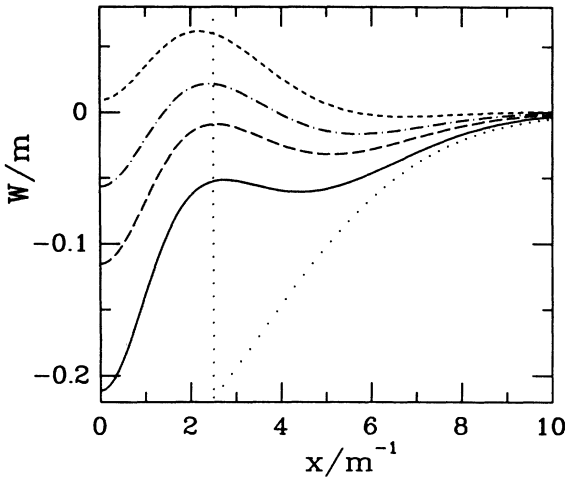

FIG. 3. The energy-dependent potential $W(x)$ for model B and U_{NR} for model C. The upper four curves are for the W's for four different energies; $E/m=2.0$, 2.1, 2.168, and 2.25 (from bottom to top). At $E/m=2.168$, the phase shift changes sign. The dotted line depicts U_{NR}. Note that the vertical scale differs between Figs. 2 and 3.

crease with increasing energy. It is clear that fitting the empirical phase shift does not differentiate models A and B. If we were to use more general functional forms for the potentials, these curves could be made indistinguishable from the empirical $^3S_1$ NN phase shift.

Figure 2 shows the energy-dependent potential W defined by Eq. (2.7) for model A for various values of the energy; the nonrelativistic potential $U_{NR}(x)$ of model C is also shown for comparison. Figure 3 shows the same for model B. The potential W depends strongly on energy; it changes from attraction to repulsion as the energy increases, and the switch over from attraction to repulsion takes place approximately at the energy for which the phase shift changes sign from positive to negative. The mechanism of the sign change of the phase shift in the relativistic models is therefore quite different from that for the nonrelativistic model. A close examination of Eq. (2.7) shows that, as the energy E increases, the effect of S is reduced and that of V enhanced. In order to have such strong energy dependence of W it is crucial that S and V are individually very strong while $S+V$ is rather weak.

It should be noted that the W's for A and B are very different from each other and that they are both very different from the nonrelativistic potential $U_{NR}(x)$ of model C. The deuteron structure in the relativistic models is determined by the W at the deuteron energy $E=1.998m$. This W is indistinguishable from the W at $E=2m$ which is shown in Figs. 2 and 3. Note that W

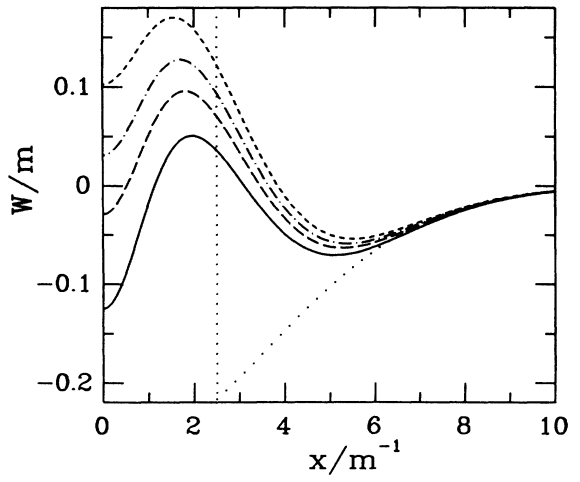

FIG. 2. The energy-dependent potential $W(x)$ for model A and U_{NR} for model C. The upper four curves are for the W's for four different energies; $E/m=2.0$, 2.1, 2.166, and 2.25 (from bottom to top). At $E/m=2.166$, the phase shift changes sign. The dotted line depicts U_{NR}.

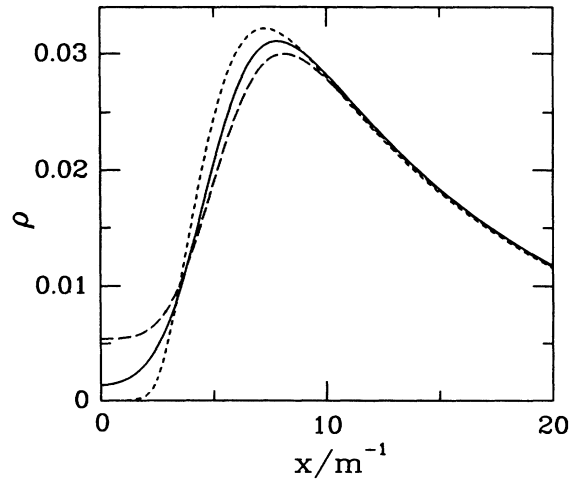

FIG. 4. The density distribution $\rho(x)$ in the deuteron in units of mass m. The solid, dashed, and short-dashed lines are for models A, B, and C, respectively.

TABLE III. The root mean square radius r_m in units of m^{-1}.

Model	A	B	C	A'	B'	C'
r_m	9.84	9.80	9.77	8.28	8.11	8.24

($E=2m$) is entirely attractive in model B, whereas it has a mild repulsive part at short distances in model A. Potential $U_{\rm NR}$ is typical of the realistic potentials which are in common use. It consists of a strong attraction at large to medium distances and a very strong repulsion at short distances.

Figure 4 shows the density distribution in the deuteron for models A, B, and C. The density does not vanish at $x=0$ in the relativistic models. This is because of the term with $|d\phi_2/dx|^2$ of Eq. (2.4). The difference between the densities of models A and B at short distances is an outcome of the difference between the W's discussed above. The densities in models A and B are appreciably different from that in model C. Table III lists the values of the root mean square radius $r_m=\langle(x/2)^2\rangle^{1/2}$ of the deuteron for models $A,B,\ldots,C'$. Because the potentials for models A, B, and C are very different, one might expect that r_m varies appreciably from one model to another. On the contrary, we find that r_m remains almost the same; it decreases only very slightly from A to B and then to C. In order to examine the properties of the deuteron in detail, however, one must fine tune the potential such that the scattering data are more accurately fitted.

The differences between the models will manifest themselves through the deuteron form factor (at not very small momentum transfers) rather than through r_m. Let us define the form factor as the Fourier transform of the density,

$$F(q^2)=\int_{-\infty}^{\infty} dx\,\rho(x)e^{iqx}=2\int_0^{\infty} dx\,\rho(x)\cos qx\ . \qquad (3.1)$$

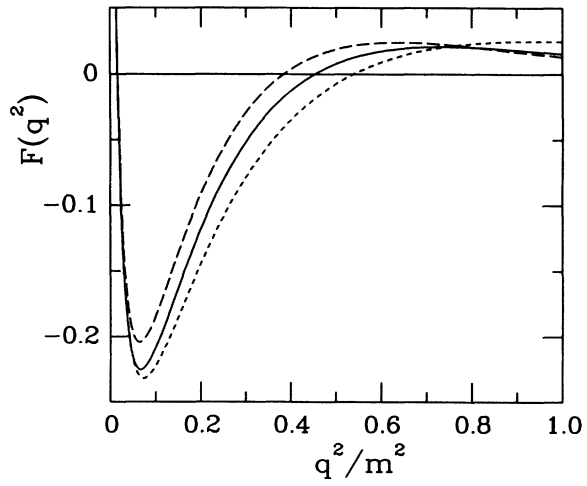

FIG. 5. The form factor $F(q^2)$ defined by Eq. (3.1). The solid, dashed, and short-dashed lines are for models A, B, and C, respectively.

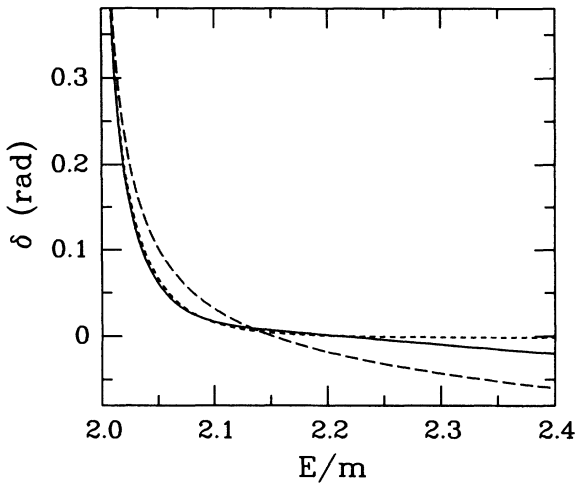

FIG. 6. The even-parity phase shift $\delta(E)$. The solid, dashed, and short-dashed lines are for models A', B', and C', respectively.

Figure 5 shows $F(q^2)$ for models A, B, and C. It is clear that the differences between the models are noticeable for $q^2\gtrsim 0.1m^2$. Note that $F(q^2)$ defined above corresponds to $F_{\rm st}(q^2)$ of Ref. 2. There is a small relativistic correction to the form factor as pointed out in Ref. 2, but we do not discuss it here.

The results of the simulation by means of the even-parity state are presented in Figs. 6–9. Figure 6 shows the phase shifts. Unlike the odd-parity case, the even-parity phase shifts start with $\pi/2$ at the threshold.[7] This is because of the boundary condition on the even-parity wave function at the origin, which is different from that on the odd-parity wave function. Clearly such a phase shift is unsuitable for simulating the $^3S_1$ NN phase shift which starts with π. This is the main reason why we

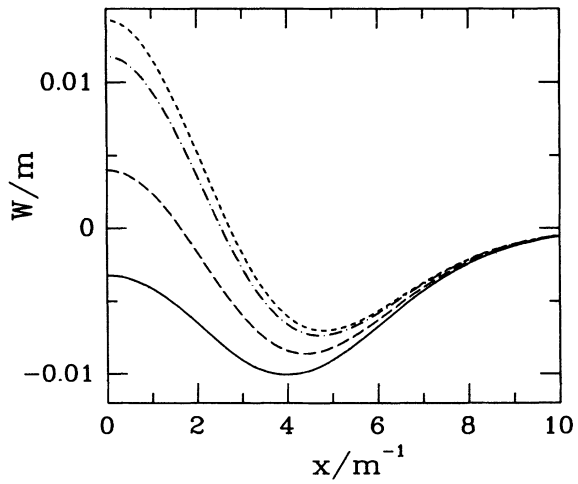

FIG. 7. The energy-dependent potential $W(x)$ for model A'. The curves are for the W's for four different energies; $E/m=2.0$, 2.1, 2.213, and 2.25 (from bottom to top). At $E/m=2.213$, the phase shift changes sign.

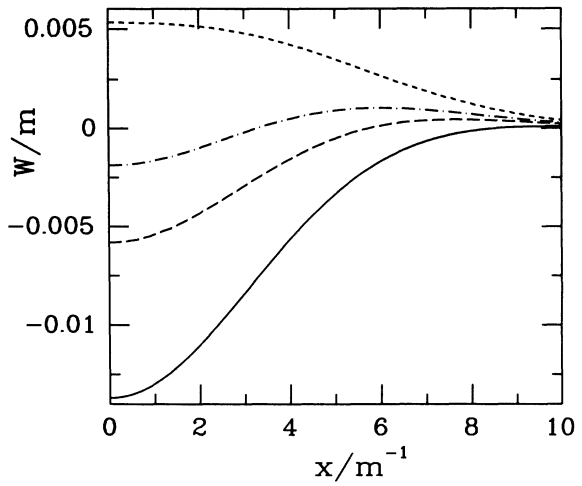

FIG. 8. The energy-dependent potential $W(x)$ for model B'. The curves are for the W's for four different energies; $E/m=2.0$, 2.1, 2.152, and 2.25 (from bottom to top). At $E/m=2.152$, the phase shift changes sign. Note that the vertical scale differs between Figs. 7 and 8.

prefer the simulation by means of the odd-parity state. The phase shift for model B' is rather different from those of models A' and C'. We did not try hard to make them closer.

Figures 7 and 8 show the energy-dependent potential W for models A' and B', respectively. Note that these potentials are much weaker than those for the odd-parity state. In the even-parity state such very weak potentials are capable of supporting a bound state. This is another reason why the even-parity state is unsuitable for simulating the $^3S_1$ NN system. Figure 9 shows the density distribution in the deuteron for models A', B', and C'.

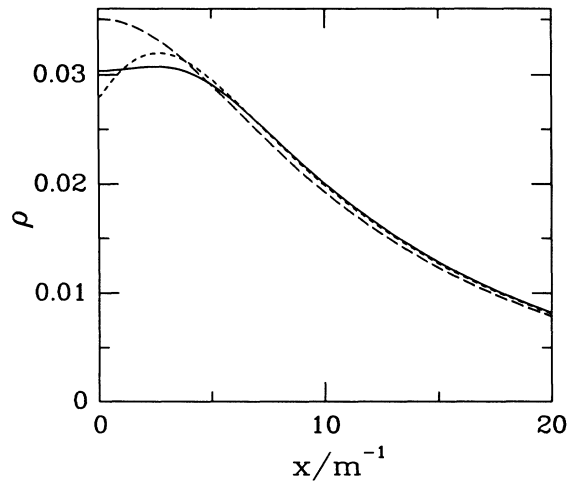

FIG. 9. The density distribution $\rho(x)$ in the deuteron in units of mass m. The solid, dashed, and short-dashed lines are for models A', B', and C'.

IV. DISCUSSIONS

By means of one-dimensional models which simulate the deuteron and $^3S_1$ NN scattering, we have illustrated characteristic differences between relativistic and nonrelativistic treatments. The relativistic interaction can be transcribed into an effective potential W for the Schrödinger-like equation (2.6). This W turned out to be strongly energy dependent. This is due to the particular combination of S and V such that S and V are individually very strong while $S+V$ is much weaker. This energy dependence of W is the main mechanism behind the sign change of the phase shift (from positive to negative) in the relativistic models. This feature, i.e., the strong energy dependence of the relativistic interaction, will certainly remain valid when the dimension is increased from one to three. In the nonrelativistic treatment, the sign change of the phase shift requires a combination of a short-range repulsion and a long-range attraction. In the relativistic case the ratio of the ranges of S and V, a_S/a_V, has large latitude. Depending on this ratio, W varies significantly. The variation of W, in turn, is reflected in the structure of the deuteron. We examined the form factor $F(q^2)$ defined by Eq. (3.1) and found that the differences between the models are detectable through $F(q^2)$ at $q^2 \gtrsim 0.1m^2$. We should note, however, that there is a subtle difference between one and three dimensions. The $F(q^2)$ of Eq. (3.1) can be expanded as

$$\Sigma(-1)^n q^{2n}\langle x^{2n}\rangle/(2n)!\ ,$$

whereas its three-dimensional counterpart is

$$\Sigma(-1)^n q^{2n}\langle r^{2n}\rangle/(2n+1)!\ .$$

This means that the $F(q^2)$ of one dimension corresponds to the three-dimensional $F(q^2)$ with a larger value of q^2.

If one assumes that the NN interaction derives from meson exchanges, the ranges of S and V are related to the masses of scalar and vector mesons, respectively. For the vector meson, ω and ρ are the natural choice, but there is no such clear candidate for the scalar part. It is interesting in this respect that there is large arbitrariness regarding the range of S.

As compared with the usual nonrelativistic NN potentials, relativistic interactions at low energies are much softer, particularly at short distances. They are comparable or softer than the super-soft potential of Srivastava *et al.*[8] They may have significant consequences regarding many-nucleon systems. For infinite nuclear matter, for example, the relativistic models could lead to a saturation density larger than that obtained from nonrelativistic calculations. This is interesting in view of the failure of all nonrelativistic models in reproducing the "empirical" values of the saturation density and the binding energy of infinite nuclear matter.[9,10] In this connection let us mention that Satpathy recently raised a question about the reliability of the traditional values of the empirical saturation density and binding energy of nuclear matter.[11]

In our relativistic models we considered only the com-

bination of a Lorentz scalar and a vector. In the actual NN interaction there is a pseudoscalar component which contains the one-pion-exchange (OPE) effect. The OPE potential is not a very strong part of the nonrelativistic potential, but this does not necessarily mean that the pseudoscalar component is unimportant in the relativistic interaction. Rather we suspect that the pseudoscalar component could be as important as S and V. In the limit of a very large nucleon mass, the effective potential W still reduces to $S+V$, and the effect of the pseudoscalar component begins to operate in the order of m^{-1}, but if the mass is not very large (as compared with the potentials), the effect of the pseudoscalar interaction could be significant. In a more realistic model of the relativistic NN interaction one must include a pseudoscalar component.

The two-body Dirac equation that we have used is not exactly covariant. Also the equation has abnormal bound-state solutions (with $E \approx 0$) as discussed in detail recently.[3] However, the energy region ($E \gtrsim 2m$) that we are concerned with is very far from the region in which abnormal solutions show up. We therefore believe that the two-body Dirac equation adequately describes "low-energy" phenomena such as those discussed in this paper.

ACKNOWLEDGMENTS

We would like to thank Dr. D. W. L. Sprung and Dr. W. van Dijk for helpful comments. This work was supported by the Natural Sciences and Engineering Research Council of Canada.

---

*On leave from Institute of Computer Sciences, Kyoto Sangyo University, Kyoto 603, Japan.

[1]In addition all of these realistic potentials have the one-pion-exchange-potential tail.

[2]W. Glöckle, Y. Nogami, and I. Fukui, Phys. Rev. D **35**, 584 (1987).

[3]F. A. B. Coutinho, W. Glöckle, Y. Nogami, and F. M. Toyama, Can. J. Phys. (in press).

[4]For other references see those quoted in Ref. 2.

[5]J. A. McNeil, J. R. Shepard, and S. J. Wallace, Phys. Rev. Lett. **50**, 1439 (1983); J. R. Shepard, J. A. McNeil, and S. J. Wallace, *ibid.* **50**, 1443 (1983); B. C. Clark, S. Hama, R. L. Mercer, L. Ray, and B. D. Serot, *ibid.* **50**, 1644 (1983).

[6]Of course we could have used the actual values of the nucleon mass (939 MeV) and the deuteron binding energy (2.225 MeV). Since we are doing a simulation, we opted for neat schematic numbers. We did not attempt to fit the $^3S_1$ NN phase shift and the root mean square radius of the deuteron exactly.

[7]For the definition of the phase shift in one dimension we follow J. H. Eberly, Am. J. Phys. **33**, 771 (1965).

[8]M. K. Srivastava, P. K. Banerjee, and D. W. L. Sprung, Phys. Lett. **29B**, 635 (1969). They considered only the $^1S_0$ state though.

[9]D. Day, Comments Nucl. Part. **11**, 115 (1983); Phys. Rev. Lett. **47**, 226 (1981); Phys. Rev. C **24**, 1203 (1984).

[10]See, however, R. Brockmann and R. Machleidt, Phys. Lett. **149B**, 283 (1984). They pointed out that a self-consistent treatment of the relativistic nucleon wave function in nuclear matter results in repulsive effects, which are absent in nonrelativistic theories. This may compensate for the softness of the potential that we pointed out.

[11]L. Satpathy, J. Phys. G **13**, 761 (1987).